Kinetic and Chemical Mechanism of *Mycobacterium tuberculosis* 1-Deoxy-D-xylulose-5-phosphate Isomeroreductase†

Argyrides Argyrou* and John S. Blanchard

Department of Biochemistry, Albert Einstein College of Medicine, 1300 Morris Park Avenue, Bronx, New York 10461

Received January 2, 2004; Revised Manuscript Received February 12, 2004

ABSTRACT: 1-Deoxy-D-xylulose-5-phosphate (DXP) isomeroreductase catalyzes the isomerization and reduced nicotinamide adenine dinucleotide phosphate- (NADPH-) dependent reduction of DXP to generate 2-*C*-methylerythritol 4-phosphate (MEP) in the first committed step of the MEP pathway of isoprenoid biosynthesis. We have cloned the gene encoding the *Mycobacterium tuberculosis* DXP isomeroreductase, expressed the protein in *Escherichia coli*, and purified the enzyme to homogeneity using conventional column chromatography methods. DXP isomeroreductase is a metal ion-activated enzyme displaying superior specificity for Co^{2+}, good specificity for Mn^{2+}, and poor specificity for Mg^{2+}. Although NADPH is preferred over reduced nicotinamide adenine dinucleotide (NADH) about 100-fold as evaluated by the relative k_{cat}/K_m values, the maximum turnover numbers are similar, suggesting that the 2′-phosphate of NADPH contributes predominantly to binding and not to catalysis. While k_{cat} was independent of pH in the region $6.0 \leq pH \leq 8.75$, $k_{cat}/K_{act}^{Mn^{2+}}$ decreased at low pH as two enzymatic groups with pK_a values of 7.4 are protonated. These groups likely represent carboxylate groups that coordinate the divalent metal ion in the active site. The results also support an electrostatic role for the divalent metal ion in catalysis. The results of product inhibition studies and isotope effects suggest that the enzyme utilizes a steady-state random mechanism. Significant isotope effects were observed with [4*S*-^{2}H]NAD(P)H, establishing that the enzyme promotes transfer of the C_4-*proS* hydride of the reduced pyridine nucleotide. The magnitude of these primary deuterium kinetic isotope effects varied with metal ion and reduced pyridine nucleotide identities. The results are discussed in terms of significant differences in the commitment factors for the various metal ions and pyridine nucleotides.

Isopentenyl pyrophosphate (IPP)[1] and dimethylallyl pyrophosphate (DMAPP) are the building blocks for approximately 23 000 isoprenoid compounds (*1*). Until the early 1990s, the mevalonate pathway was thought to be the universal pathway leading to formation of IPP and DMAPP. It is now known that enzymes of the mevalonate pathway, present in animal cells and the cytosol of plant cells, are absent from algae, plant plastids, and most eubacteria, which instead use the 2-*C*-methylerythritol 4-phosphate (MEP) pathway (Scheme 1) (*2*, *3*). The MEP pathway enzymes are also present in the apicoplast of the malarial parasite *Plasmodium falciparum* (*4*, *5*). Since these two pathways utilize completely different enzymes and substrates, any inhibitor of the MEP pathway in pathogenic bacteria is expected to have little, if any, toxic effect in humans. Some of these isoprenoid compounds are critical for cell viability, and in bacteria examples include bactoprenol, required in cell wall construction, and ubiquinone, important in oxidative metabolism.

The MEP pathway (Scheme 1) begins with the isomerization and pyridine nucleotide-dependent reduction of 1-deoxy-D-xylulose-5-phosphate (DXP) to generate MEP, catalyzed by the *dxr*-encoded (also known as *ispC*) DXP isomeroreductase (also known as DXP reductoisomerase or MEP synthase). MEP is subsequently converted to IPP and DMAPP after cytidylylation, phosphorylation, cyclization, and two more enzymatic steps, each involving reduction and dehydration. DXP, the product of a condensation reaction between pyruvate and D-glyceraldehyde 3-phosphate, catalyzed by the thiamin diphosphate- (TDP-) dependent enzyme DXP synthase (*6*), is also a metabolic precursor of pyridoxal phosphate (*7*, *8*) and the thiazole ring of thiamin diphosphate (*9*), two important cofactors for many metabolic enzymes.

The importance of the MEP pathway is highlighted by the identification of fosmidomycin (Scheme 2), a naturally occurring antibiotic, whose target has been shown to be DXP isomeroreductase (*10*). Fosmidomycin is bacteriostatic against the in vitro growth of *Escherichia coli* with a minimum inhibitory concentration of 3 μg/mL (*10*), it can cure mice infected with *Plasmodium vinckei* (*4*), and it is well tolerated in humans (*11*). Knockouts of DXP isomeroreductase in *E. coli* (*12*, *13*) and *Bacillus subtilis* (*14*) are lethal. In

† Supported by NIH Grant GM33449.

* Corresponding author: tel (718) 430-3097; fax (718) 430-8565; e-mail aargyrou@medusa.bioc.aecom.yu.edu.

[1] Abbreviations: ATP, adenosine 5′-triphosphate; DMAPP, dimethylallyl pyrophosphate; DXP, 1-deoxy-D-xylulose-5-phosphate; Hepes, *N*-(2-hydroxyethyl)piperazine-*N*′-(2-ethanesulfonic acid); IPP, isopentenyl pyrophosphate; IPTG, isopropyl 1-thio-β-D-galactopyranoside; MEP, 2-*C*-methyl-D-erythritol 4-phosphate; Mes, 2-(*N*-morpholino)-ethanesulfonic acid; NAD(P)H, reduced β-nicotinamide adenine dinucleotide (phosphate); $NAD(P)^+$, oxidized β-nicotinamide adenine dinucleotide (phosphate); PCR, polymerase chain reaction; SDS−PAGE, sodium dodecyl sulfate−polyacrylamide gel electrophoresis; Taps, *N*-tris(hydroxymethyl)methyl-3-aminopropanesulfonic acid; TDP, thiamin diphosphate; TEA, triethanolamine; Tris, tris(hydroxylmethyl)-aminomethane.

10.1021/bi049974k CCC: $27.50
Published on Web 03/16/2004

Scheme 1: MEP Pathway

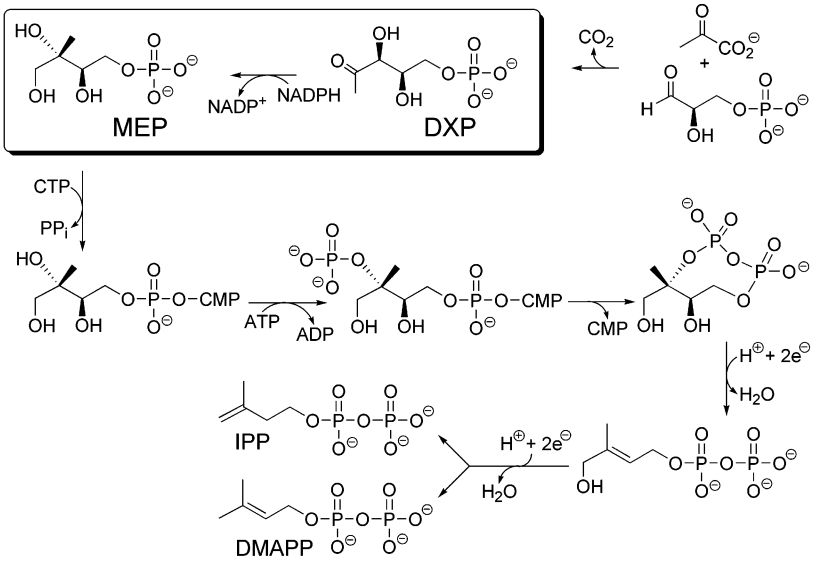

Scheme 2: Possible Mechanisms for DXP Isomeroreductase

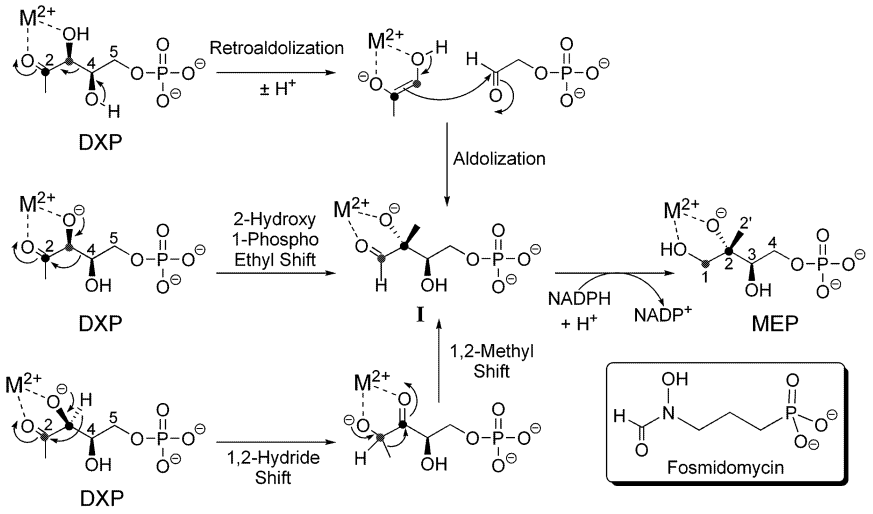

B. subtilis, all enzymes in the MEP pathway are essential (*14*). Our research group has been interested in developing enzymes involved in critical biosynthetic pathways into targets for inhibitor design, with more emphasis on enzymes in the human pathogen *Mycobacterium tuberculosis*. The *M. tuberculosis* genome encodes putative orthologues of all the enzymes in the MEP pathway and no apparent orthologues of the mevalonate pathway (*2*). We, therefore, think that the enzymes in the MEP pathway are appropriate targets for inhibitor design in *M. tuberculosis*.

DXP isomeroreductase catalyzes one of the most unusual reactions in biological chemistry. The divalent metal ion-dependent reaction is composed of consecutive isomerization and reduction steps. Formation of the 2-*C*-methylerythrose 4-phosphate intermediate (**I**, Scheme 2) from DXP could proceed in three different ways: (1) oxidation of the 3-hydroxyl group to the corresponding ketone while the 1-hydroxy-2-phosphoethyl moiety is transferred to the C_2 ketone (middle pathway, Scheme 2) (*15*, *16*); (2) oxidation of the 4-hydroxyl group concomitant with C_3–C_4 bond scission to generate the enol/enolate of 3-hydroxyacetone and glycoaldehyde 3-phosphate, followed by recombination of these two moieties via C_2 of 3-hydroxyacetone (upper pathway, Scheme 2) (*17*); or (3) sequential 1,2-hydride and 1,2-methyl shifts (lower pathway, Scheme 2). NADPH then reduces the C_1 aldehyde of **I** to a primary alcohol to generate MEP.

In this paper, we describe the cloning, expression of the protein in *E. coli*, and purification of DXP isomeroreductase from *M. tuberculosis*. We have determined the steady-state kinetic parameters for the forward and reverse directions, defined the metal ion specificity, explored the steady-state kinetic mechanism, probed for the presence of general acid/base catalysts using pH−rate profiles, and begun probing rate-limiting steps using primary deuterium kinetic isotope effects.

EXPERIMENTAL PROCEDURES

Materials. All chemicals were of analytical or reagent grade and were used without further purification unless otherwise stated. ATP, D-fructose 1,6-bisphosphate, D-(+)-glucose, NADPH, $NADP^+$, NADH, sodium pyruvate, thiamin diphosphate, rabbit muscle aldolase, rabbit muscle triosephosphate isomerase (type X), *Thermoplasma acidophilum* glucose dehydrogenase, *Leuconostoc mesenteroides* glucose-6-phosphate dehydrogenase (type XXIV), and yeast

hexokinase (type C-300) were from Sigma. 2-[^{13}C]Pyruvate (99 atom % ^{13}C) was from Cambridge Isotope Laboratories. D-Glucose-1-*d* (97 atom % D) was from Aldrich. All restriction enzymes, calf intestinal phosphatase, and T4 DNA ligase were obtained from New England Biolabs.

General Methods. Protein concentrations were determined with bicinchoninic acid (*18*) with bovine serum albumin as standard. Solution pH values were measured at 25 °C with an Accumet model 20 pH meter and Accumet combination electrode standardized at pH 7.00 and 4.00 or 10.00. Spectrophotometric assays were performed on a Uvikon XL double-beam UV−vis spectrophotometer (Bio-Tek Instruments).

Cloning and Expression. The genes encoding DXP isomeroreductase (Rv2870c, *dxr*) from *M. tuberculosis* and DXP synthase (*dxs*) from *E. coli* were amplified by PCR to generate blunt-ended DNA with *Nde*I and *Hin*dIII or with *Nde*I and *Xho*I restriction sites at the ends, respectively. The oligonucleotide primers were 5′-ATTCCATATGACCAACTCGACCGACGGGCG-3′ and 5′-CCCAAGCTTTCAGGACCTTTCTAACGTCGA-3′ (for *dxr*) and 5′-CATATG-(CATCAC)$_3$ATGAGTTTTGATATTGCCAAATACCCG-3′ and 5′-CTCGAGTTATGCCAGCCAGGCCTTGATTTTGGCTTCCATACCGGC-3′ (for *dxs*). The amplified DNA product was ligated into the pCR-Blunt plasmid and transformed into One Shot TOP10 cells following the instructions supplied by the manufacturer (Invitrogen). Plasmid DNA isolated from these cells was then digested with the above restriction enzymes and the purified insert was ligated into purified plasmid pET-23a(+) (Novagen) previously linearized with the same restriction enzymes. This recombinant plasmid was then transformed into competent *E. coli* BL21(DE3) cells (Novagen). The BL21(DE3) cells containing the recombinant plasmid were grown at 37 °C to an A_{600nm} of 0.7 in Luria−Bertani medium containing 50 μg/mL ampicillin. The cells were then cooled to 20 °C and temperature-equilibrated for 2 h, and protein expression was induced by the addition of 0.5 mM IPTG and allowed to proceed for 16 h at 20 °C. DNA sequencing of the cloned *dxr* and *dxs* genes showed that they were free of mutations.

Purification of Enzymes. All operations were carried out at 4 °C. Cell paste (30−40 g) was suspended in 20 mM TEA, pH 7.8 (100 mL, final volume), containing three tablets of Complete protease inhibitor cocktail (Boehringer Mannheim), 50 mg of chicken egg white lysozyme (Sigma), 10 mg of bovine pancreatic DNase I (Boehringer Mannheim), and 10 mM $MgCl_2$ and stirred for 30 min. The cells were disrupted by sonication and cell debris was removed by centrifugation at 20000*g* for 60 min. The supernatant, referred to below as crude soluble extract, was treated as described.

DXP Synthase. Buffers were supplemented with 0.5 mM TDP. The crude soluble extract was applied to a 50 mL column of Ni−NTA His·Bind Superflow (Novagen) equilibrated with buffer A (20 mM TEA, pH 7.8, and 5 mM $MgCl_2$) containing 0.3 M NaCl. The column was washed with 150 mL of the same buffer and eluted with a linear gradient (400 mL) from 0 to 0.25 M imidazole in buffer A also containing 0.3 M NaCl. The fractions containing DXP synthase were pooled and dialyzed against 4 L of buffer A, and the enzyme was concentrated to 10 mL and stored at −20 °C in 50% glycerol.

DXP Isomeroreductase. The crude soluble extract was dialyzed for 4 h against 4 L of buffer A and the precipitate, which formed during dialysis, was removed by centrifugation as above. The dialysate (110 mL) was applied to a 70 mL column of Q-Sepharose FF (Amersham−Pharmacia Biotech) equilibrated with buffer A. The column was washed with 200 mL of the same buffer and then eluted with a linear gradient (800 mL) from 0 to 0.6 M NaCl in buffer A. The fractions containing DXP isomeroreductase, which eluted at 0.2−0.3 M NaCl, were pooled and concentrated to 35 mL. Ammonium sulfate was then added to a final concentration of 0.3 M. The supernatant, after centrifugation as above, was applied to a 100 mL column of phenyl-Sepharose HP (Amersham−Pharmacia Biotech) equilibrated with buffer A containing 0.3 M ammonium sulfate. The column was washed with 200 mL of the same buffer and then eluted with a linear reverse gradient (800 mL) from 0.3 to 0 M ammonium sulfate. The fractions containing DXP isomeroreductase were pooled, concentrated to 4 mL, and applied to a calibrated 320 mL HiTrap Sephacryl S-200 HR column (Amersham−Pharmacia Biotech), equilibrated with buffer A. DXP isomeroreductase eluted as a dimer. Finally, the fractions containing the enzyme were applied to a 25 mL Mono-Q column (Amersham−Pharmacia Biotech) equilibrated with buffer A and were eluted with a linear gradient (600 mL) from 0 to 0.6 M NaCl in buffer A. DXP isomeroreductase eluted in three peaks (peak I, ∼0.2 M NaCl; peak II, ∼0.25 M NaCl; and peak III, ∼0.3 M NaCl) and all three were active. The three peaks were kept separate. Each was dialyzed against buffer A, concentrated to ∼5 mg mL^{-1}, and stored at −20 °C in 50% glycerol, with no detectable loss of activity for over a year. Electrospray ionization/mass spectrometry showed a subunit molecular mass of 42 719 Da (peak I), equal proportions of two species with molecular masses of 42 722 and 40 936 Da (peak II), and 40 938 Da (peak III), compared to 42 722 Da expected for full-length *dxr* with the N-terminal methionine posttranslationally removed (see Results). A total of 20 mg of pure protein was obtained from 30 g of cell paste.

Synthesis and Purification of DXP. DXP was synthesized enzymatically by *E. coli* DXP synthase from pyruvate and D-glyceraldehyde 3-phosphate, which was generated in situ by the action of aldolase on D-fructose 1,6-bisphosphate, as described previously (*19*). D-Fructose 1,6-bisphosphate (102 mg) and 55 mg of sodium pyruvate (or 2-[^{13}C]pyruvate) were dissolved in 10 mL of 50 mM Tris, pH 7.5, containing 1 mM TDP, 1 mM DTT, and 5 mM $MgCl_2$. Triosephosphate isomerase (50 units), aldolase (10 units), and purified DXP synthase were then added and the reaction was allowed to proceed at 37 °C for ∼20 h. The reaction, after removal of the enzymes by ultrafiltration through a YM10 membrane (Millipore), was then applied to a 20 mL Dowex 1 × 8 column (formate form), washed with 100 mL of water, and eluted with 1 M formic acid. The fractions containing pure DXP were pooled and the solvent was evaporated on a rotary evaporator under vacuum. DXP was then dissolved in water, the pH was adjusted to 6.5 with sodium hydroxide, and the sample was stored at −20 °C.

Synthesis and Purification of MEP. MEP was also synthesized enzymatically by purified *M. tuberculosis* DXP isomeroreductase, enzymatically synthesized DXP (above), and NADPH. Tris, pH 7.5 (50 mM), 10 mM $MgCl_2$, 25 mM DXP (or 10 mM 2-[^{13}C]DXP), 0.2 mM $NADP^+$, 100 mM D-(+)-glucose, 53 units of *Thermoplasma acidophilum*

glucose dehydrogenase, and 2 μM *M. tuberculosis* DXP isomeroreductase in a 5 mL reaction were incubated for 24 h at 25 °C. The reaction, after removal of the enzymes by ultrafiltration through a YM10 membrane (Millipore), was then applied to a 20 mL Dowex 1 × 8 (formate form) column, washed with 100 mL of water, and eluted with 1 M formic acid (*20*). The fractions containing pure MEP were pooled and the solvent was evaporated on a rotary evaporator under vacuum. MEP was then dissolved in water, the pH was adjusted to 6.5, and the sample was stored at −20 °C.

Determination of DXP and MEP Concentrations. Aliquots of DXP and MEP were dephosphorylated completely by calf instestinal phosphatase, and the released inorganic phosphate was quantitated as described (*21*). ^{1}H NMR, with a known concentration of glycine as an internal standard, confirmed the precision of this method.

Preparation of [4S-^{2}H]NAD(P)H. [4*S*-^{2}H]NAD(P)H was prepared by enzymatic reduction of the oxidized pyridine nucleotide with *Leuconostoc mesenteroides* (type XXIV) glucose-6-phosphate dehydrogenase with [1-^{2}H]glucose 6-phosphate as the deuterium source as described previously (*22*). [4*S*-^{2}H]NAD(P)H and nondeuterated NAD(P)H were purified on a Mono-Q column (Amersham−Pharmacia Biotech) as described previously (*23*), and the fractions with absorbance ratios $A_{260nm}/A_{340nm} \leq 2.3$ were pooled.

Assay for DXP Isomeroreductase. All assays were performed at 25 °C under initial rate conditions. The NAD(P)H-dependent isomerization and reduction of DXP catalyzed by DXP isomeroreductase was assayed spectrophotometrically at 340 nm ($\epsilon_{340nm} = 6220$ M^{-1} cm^{-1}) or 370 nm ($\epsilon_{370nm} = 2400$ M^{-1} cm^{-1}) associated with the oxidation of NAD(P)H.

Data Analysis. Data were fitted with the nonlinear least-squares curve-fitting programs of SigmaPlot 2000 for Windows version 6.00 (SPSS Inc.). Individual saturation curves were fitted to

$$v = VA/(A + K) \quad (1)$$

where V is the maximal velocity, A is the substrate concentration, and K is the Michaelis constant (K_m). Data showing intersecting initial velocity patterns on reciprocal plots were fitted to

$$v = VAB/(K_{ia}K_B + K_AB + K_BA + AB) \quad (2)$$

where A and B are the concentrations and K_A and K_B are the Michaelis constants for the substrates. Data displaying competitive and noncompetitive inhibition were fitted to eqs 3 and 4, respectively, where I is the inhibitor concentration, and K_{is} and K_{ii} are inhibition constants:

$$v = VA/[K(1 + I/K_{is}) + A] \quad (3)$$

$$v = VA/[K(1 + I/K_{is}) + A(1 + I/K_{ii})] \quad (4)$$

Primary deuterium kinetic isotope effect experiments were performed at a saturating concentration of the cosubstrate ($\geq 20K_m$) and were calculated from

$$v = VA/[K(1 + F_iE_{V/K}) + A(1 + F_iE_V)] \quad (5)$$

where $E_{V/K}$ and E_V are the isotope effects minus 1 on V/K and V, respectively, and F_i is the fraction of isotopic label. With NADH as reductant, it was not possible to saturate the enzyme with the cosubstrate because of the high K_m values. To determine the isotope effects, we varied one substrate at five fixed levels of the cosubstrate. The resulting 50 data points (25 for NADH and 25 for [4*S*-^{2}H]NADH) were simultaneously fitted to (*24*)

$$v = VAB/[[K_{ia}K_B(1 + F_iE_{K_{ia}}) + K_BA](1 + F_iE_{V/K_B}) + K_AB(1 + F_iE_{V/K_A}) + AB(1 + F_iE_V)] \quad (6)$$

The pH−$k_{cat}/K_{act}^{Mn^{2+}}$ profile (Figure 4) was analyzed from the goodness of the fits of the data to eqs 7 and 8, where y is $k_{cat}/K_{act}^{Mn^{2+}}$, C is the pH-independent value of $k_{cat}/K_{act}^{Mn^{2+}}$, H is [H$^+$], and K represents the observed dissociation constant(s) for group(s) on the enzyme:

$$\log y = \log C/(1 + H/K) \quad (7)$$

$$\log y = \log C/(1 + H^2/K^2) \quad (8)$$

Errors were propagated as described in Skoog and West (*25*) for indeterminate errors.

RESULTS

Cloning, Expression, Purification, and Biophysical Characterization of M. tuberculosis DXP isomeroreductase. Using the *E. coli* DXP isomeroreductase amino acid sequence as a query, we searched the *M. tuberculosis* genome for the orthologous enzyme. We identified an open reading frame (*dxr*, Rv2870c) showing 43% identity in amino acid sequence with the *E. coli* enzyme. We cloned the gene into plasmid pET23a(+), expressed the protein in *E. coli*, and purified the enzyme to homogeneity (Experimental Procedures).

The final purification step involved high-resolution Mono-Q anion-exchange chromatography, where the enzyme eluted in three peaks. The results of electrospray ionization/mass spectrometry and gel-filtration chromatography (Experimental Procedures) suggested that the enzyme was sensitive to proteolytic cleavage, resulting in the production of three enzyme species that could be resolved by high-resolution Mono-Q ion-exchange chromatography: (1) a full-length dimer (peak I), (2) a truncated dimer (peak III), and (3) a mixed full-length/truncated dimer (peak II). The enzyme species corresponding to the three peaks had identical specific activities, K_m values for DXP, and isotope effects (see below). The cleavage site was inferred from the mass spectrometric data to be Ala-395, resulting in a protein that was 18 amino acids shorter. This was confirmed by introducing a stop codon in place of Ser-396, which resulted in the exclusive production of active peak III protein (data not shown). We conclude that removal of the last 18 residues in *M. tuberculosis* DXP isomeroreductase has no effect on enzyme activity, affinity for substrates, sensitivity to isotopic probes, or oligomeric state of the protein. Amino acid sequence alignments reveal that DXP isomeroreductases from most species lack this C-terminal extension. The possible role of this C-terminal tail, which appears to be limited to mycobacterial species (*M. tuberculosis*, *Mycobacterium bovis* BCG, *Mycobacterium leprae*, and *Mycobacterium smegmatis*), is not clear at this time.

Enzyme Stability. We have noticed a significant loss of specific activity of the enzyme during purification (estimated half-life of ∼3 days at 4 °C). As a result of the lengthy

Table 1: Divalent Metal Ion Specificity of DXP Isomeroreductase[a]

metal ion	organism	K_{act}[b] (μM)	k_{cat}/K_{act} (M^{-1} s^{-1})
Mg^{2+}	*M. tuberculosis*	1200 ± 100	$(1.8 \pm 0.2) \times 10^3$
Mg^{2+}	*Synechocystis*	2400 ± 200[c]	
Mn^{2+}	*M. tuberculosis*	21 ± 2	$(2.4 \pm 0.2) \times 10^5$
Mn^{2+}	*Synechocystis*	15 ± 1[c]	
Co^{2+}	*M. tuberculosis*	1.2 ± 0.1	$(1.3 \pm 0.1) \times 10^6$
Co^{2+}	*Synechocystis*	10 ± 3[c]	

[a] At pH 7.5 and 25 °C. [b] K_{act} is defined as the concentration of metal ion required for half-maximal activity at saturating substrate concentrations (the concentrations of NADPH and DXP were 200 μM and 2 mM, respectively). Ca^{2+}, Ni^{2+}, and Zn^{2+} were not activators of the enzyme. [c] Data from ref *26*.

purification procedure, which took about 5 days to complete, there is a significant amount of inactive enzyme in our preparation, which we cannot remove by column chromatography and which contributes to the protein concentration we determined. It should, therefore, be emphasized that the absolute k_{cat} and k_{cat}/K_m values (Table 2) are lower limits. However, when stored in 50% glycerol at −20 °C, the enzyme has retained full activity for over a year. Hence, comparisons of k_{cat} values obtained with the various metal ions and substrate analogues are valid, as are all other reported parameters. We have yet to identify the nature of this inactivation or conditions that reverse the inactivation. Compared to the k_{cat} values determined for DXP isomeroreductases from other species, which vary from 8 to 110 s^{-1} (*26*), the k_{cat} values for the *M. tuberculosis* enzyme lie at the lower end of this range.

Metal Ion Requirements. Where different divalent metal ions have been examined, it was previously found that Mg^{2+}, Mn^{2+}, and Co^{2+} were activators for DXP isomeroreductase but Ca^{2+}, Ni^{2+}, and Zn^{2+} were not (*12*, *26*−*29*). This is also true for the *M. tuberculosis* DXP isomeroreductase. The specificity of DXP isomeroreductase for the various metal ions has only been determined for the *Synechocystis* sp. PCC6803 enzyme (*26*). To compare the metal ion specificities of the *M. tuberculosis* DXP isomeroreductase with those for the *Synechocystis* enzyme, we examined the dependence of the velocity of the reaction as a function of the concentration of the metal ion, at fixed and saturating concentrations of NADPH and DXP. The resulting hyperbolic curves (data not shown) were fitted to eq 1 to obtain a maximal rate, k_{cat}, and the parameter K_{act}, which is defined as the concentration of divalent metal ion required to half-saturate the rate. The K_{act} and k_{cat}/K_{act} parameters and those for the *Synechocystis* enzyme, obtained under similar experimental conditions, are similar except for an 8.3-fold lower $K_{act}^{Co^{2+}}$ value for the *M. tuberculosis* enzyme (see Table 1). The *M. tuberculosis* DXP isomeroreductase clearly has superior specificity for Co^{2+}, followed closely by Mn^{2+}, and very poor specificity for Mg^{2+}, as evaluated by the k_{cat}/K_{act} values. Though the specificity for Mg^{2+} is 720- and 130-fold lower than those for Co^{2+} and Mn^{2+}, respectively, Mg^{2+} may still be the physiologically relevant metal ion activator, as has been previously suggested (*26*, *29*), because the free intracellular concentration of Mg^{2+} in *E. coli* of ∼1−2 mM (*30*) is close to the K_{act} value, whereas those for Mn^{2+} of ∼0.01 μM (*31*) and Co^{2+} of <0.001 μM (*32*)[2] are considerably lower than the corresponding K_{act} values. This conclusion is, of course, tentative until intracellular metal ion concentrations in mycobacteria are determined.

Steady-State Kinetics. To determine the steady-state kinetic parameters (k_{cat} and K_m, Table 2) for the NADPH and DXP substrate pair (forward direction), and $NADP^+$ and MEP product pair (reverse direction), we used a saturating concentration of the metal ion activator and either (1) varied one substrate at a saturating concentration of the cosubstrate and fitted the resulting hyperbolic plots to eq 1 (for Mn^{2+} and Co^{2+}) or (2) varied one substrate at five fixed levels of the cosubstrate and simultaneously fitted the resulting 25 data points to eq 2 (for Mg^{2+}). When NADH and DXP were the substrate pair, method 2 was used because it was not possible to saturate the enzyme with either substrate. In all cases, a pattern of intersecting lines was observed (see, for example, Figure 2) on reciprocal plots, suggesting that the enzyme uses a sequential mechanism. We also performed product inhibition studies to obtain information concerning the order of substrate binding and release of products to and from the enzyme, respectively. These studies are summarized in Table 3.

Isotope Effects. To determine the stereospecificity of hydride transfer, obtain information concerning rate-limiting steps, and obtain more information concerning the steady-state kinetic mechanism, we measured primary deuterium kinetic isotope effects arising from deuterium substitution at the C_4-*proS* position of the dihydronicotinamide ring of NADPH and NADH (Experimental Procedures). Representative examples are illustrated in Figure 1 (for NADPH) and Figure 2 (for NADH). The presence of significant isotope effects establishes that *M. tuberculosis* DXP isomeroreductase promotes transfer of the C_4-*proS* hydride of the reduced pyridine nucleotide, as has been demonstrated earlier for the *E. coli* (*20*) and *Synechocystis* sp. PCC6803 (*33*) enzymes by labeling techniques. Figure 3 shows the dependence of the apparent isotope effect on V/K [$^D(V/K_{app})$] for one substrate as the concentration of the cosubstrate is varied. Isotope effects were measured with all three divalent metal ion activators and are summarized in Table 4.

pH Studies. To obtain information concerning the role of the divalent metal ion in catalysis and the potential involvement of general base/acid catalytic groups on the enzyme, we determined the pH dependence of k_{cat} and $k_{cat}/K_{act}^{Mn^{2+}}$ at saturating concentrations of NADPH and DXP. While the k_{cat} value is independent of pH in the region $6.0 \leq$ pH ≤ 8.75, the $K_{act}^{Mn^{2+}}$ value increases sharply at low pH. Due to interfering spectral signals resulting from the formation of manganese precipitates, it was technically difficult to determine these parameters at pH > 8.75. While the resulting pH−$k_{cat}/K_{act}^{Mn^{2+}}$ profile fits poorly to eq 7 (dotted line, Figure 4), it fits better to eq 8 as two groups with similar pK_a values of 7.4 are ionized. Though the data could be fitted even better to more complex models, we think it is preliminary to invoke such models. Therefore, we can only conclude, at this time, that at least two enzymatic groups have to be deprotonated to bind the metal ion activator in a catalytically active configuration (see Discussion).

DISCUSSION

Steady-State Kinetic Mechanism. A pattern of intersecting lines on a reciprocal plot for both the forward and reverse

[2] This value was calculated from the data of D'Souza and Holz (Table 1, ref *32*) who found that, in *E. coli*, the intracellular concentration of Mn^{2+} is at least 9-fold higher than that of Co^{2+}.

Table 2: Steady-State Kinetic Parameters for *M. tuberculosis* DXP Isomeroreductase[a]

		Forward Direction				
			NAD(P)H		DXP	
metal ion	pyridine nucleotide	k_{cat} (s^{-1})	K_m (μM)	k_{cat}/K_m ($M^{-1}\,s^{-1}$)	K_m (μM)	k_{cat}/K_m ($M^{-1}\,s^{-1}$)
Mg^{2+}	NADPH	2.1 ± 0.1	5.0 ± 1.3	$(4.2 \pm 1.2) \times 10^5$	42 ± 7	$(5.0 \pm 0.9) \times 10^4$
	NADH	2.8 ± 0.5	410 ± 140	$(6.9 \pm 2.6) \times 10^3$	210 ± 150	$(1.3 \pm 0.9) \times 10^4$
Mn^{2+}	NADPH	5.0 ± 0.1	3.3 ± 0.2	$(1.5 \pm 0.1) \times 10^6$	100 ± 4	$(5.0 \pm 0.2) \times 10^4$
	NADH	5.6 ± 0.2	260 ± 20	$(2.2 \pm 0.2) \times 10^4$	240 ± 30	$(2.4 \pm 0.3) \times 10^4$
Co^{2+}	NADPH	1.6 ± 0.1	0.4 ± 0.1[b]	$(3.6 \pm 0.6) \times 10^6$	4.0 ± 0.3	$(3.9 \pm 0.3) \times 10^5$
	NADH	2.5 ± 0.2	50 ± 10	$(5.0 \pm 1.0) \times 10^4$	50 ± 10	$(5.5 \pm 1.2) \times 10^4$
		Reverse Direction				
			$NADP^+$		MEP	
metal ion	pyridine nucleotide	k_{cat} (s^{-1})	K_m (μM)	k_{cat}/K_m ($M^{-1}\,s^{-1}$)	K_m (μM)	k_{cat}/K_m ($M^{-1}\,s^{-1}$)
Mg^{2+}	$NADP^+$	1.3 ± 0.1	170 ± 30	$(7.7 \pm 1.4) \times 10^3$	42 ± 4	$(3.2 \pm 0.3) \times 10^4$

[a] At pH 7.5 and 25 °C. The following concentrations of divalent metal ions were used: Mg^{2+}, 10 mM; Mn^{2+}, 1 mM; Co^{2+}, 1 mM. The following constants were also obtained from the analysis of the Mg^{2+} data: $K_{i(NADPH)} = 27 \pm 6$ μM, $K_{i(DXP)} = 220 \pm 70$ μM, $K_{i(MEP)} = 110 \pm 30$ μM, and $K_{i(NADP^+)} = 440 \pm 80$ μM. [b] Approaches the detection limit of the assay.

Table 3: Product Inhibition Patterns for Mg^{2+}-Activated *M. tuberculosis* DXP Isomeroreductase[a]

varied substrate	product inhibitor	pattern[b]	K_{is}	K_{ii}
NADPH[c]	$NADP^+$	NC	1.2 ± 0.1 mM	2.5 ± 0.2 mM
DXP[d]	$NADP^+$	NC	1.7 ± 0.2 mM	1.4 ± 0.1 mM
NADPH[c]	MEP	NC	160 ± 20 μM	90 ± 10 μM
DXP[d]	MEP	C	49 ± 3 μM	

[a] At pH 7.5, 10 mM Mg^{2+}, 25 °C. [b] C = competitive, NC = noncompetitive. [c] The cosubstrate, DXP, was present at a fixed and unsaturating concentration of 50 μM. [d] The cosubstrate, NADPH, was present at a fixed and unsaturating concentration of 10 μM.

directions was observed for DXP isomeroreductase from *M. tuberculosis*, suggesting that the enzyme utilizes a sequential mechanism (see, for example, Figure 2). In all cases, the lines intersected left of the *y*-axis and above the *x*-axis of these reciprocal plots, ruling out a rapid equilibrium ordered mechanism, in which the lines would intersect on the *y*-axis when the reciprocal of the concentration of the second substrate to add to the enzyme is plotted on the *x*-axis (*34*). The isotope effects, discussed below, also support this conclusion.

A classic method of obtaining information of the order of substrate binding and release of products involves product inhibition experiments. With *M. tuberculosis* DXP isomeroreductase, $NADP^+$ is noncompetitive versus both NADPH and DXP, while MEP is competitive versus DXP but noncompetitive versus NADPH (Table 3). While these results alone are compatible with an ordered mechanism with DXP binding first, followed by NADPH, and release of $NADP^+$ before MEP (*35*), such experiments are often inconclusive (*24*) and more evidence is required from independent studies. Furthermore, they are incompatible with (1) isotope effects described later and (2) the results of inhibition studies on the *E. coli* DXP isomeroreductase employing the dead-end inhibitors fosmidomycin and tetrahydronicotinamide adenine dinucleotide phosphate, which suggested an ordered kinetic mechanism with NADPH binding first and DXP second (*29*). To obtain more information regarding the steady-state kinetic mechanism, we determined how the apparent isotope effect on V/K for the varied substrate, $^D(V/K_{app})$, is influenced by

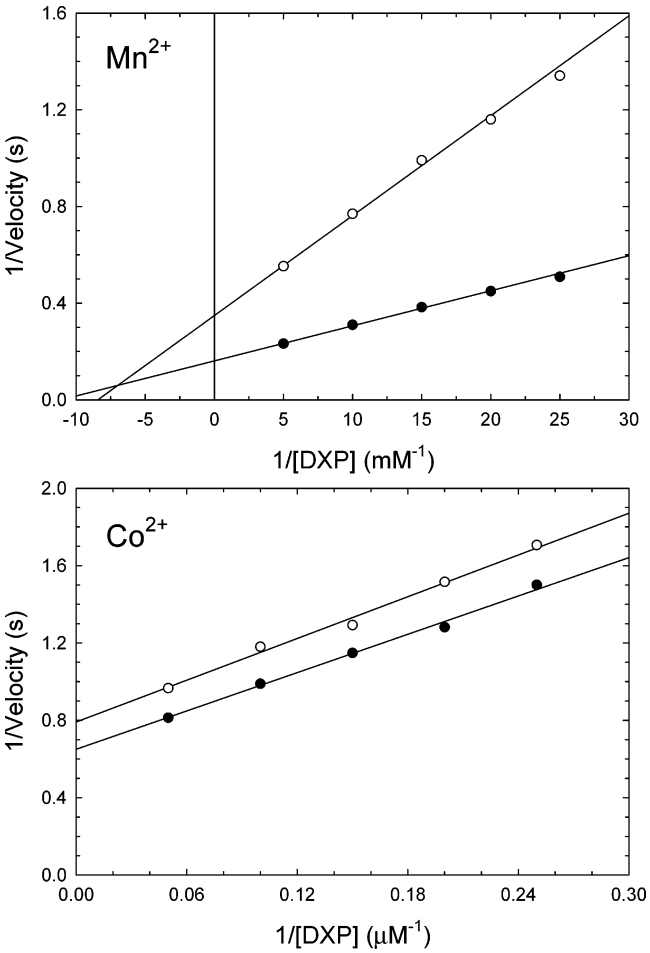

FIGURE 1: Reciprocal plots illustrating significant differences in the primary deuterium kinetic isotope effects for the Mn^{2+}- versus Co^{2+}-activated *M. tuberculosis* DXP isomeroreductase. Assays contained 100 mM Hepes, pH 7.5; 1 mM Mn^{2+} (top panel) or 1 mM Co^{2+} (bottom panel); the indicated levels of DXP; 200 μM NADPH (solid symbols) or 200 μM [4S-^{2}H]NADPH (open symbols); and *M. tuberculosis* DXP isomeroreductase. Data were fitted to eq 5.

the concentration of the cosubstrate (*24*), a powerful technique that takes advantage of the kinetic mechanism-dependent effect of cosubstrate stickiness[3] on $^D(V/K_{app})$, as described next.

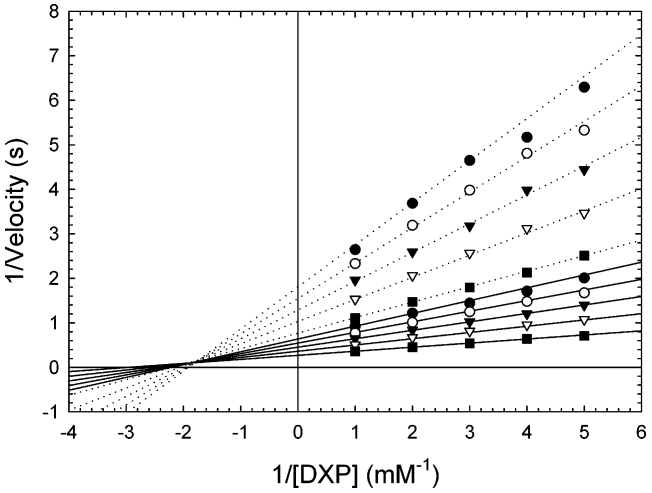

FIGURE 2: Reciprocal plot illustrating how the isotope effects for cases where substrates with high K_m values were determined. Assays contained 100 mM Hepes, pH 7.5, 1 mM Mn^{2+}, *M. tuberculosis* DXP isomeroreductase, DXP, and NADH (solid lines) or [4*S*-^{2}H]-NADH (dotted lines). DXP was varied (0.200, 0.250, 0.333, 0.500, and 1.00 mM) at five fixed levels (0.100, 0.125, 0.167, 0.250, and 0.500 mM) of NADH or [4*S*-^{2}H]NADH. The resulting 50 data points were simultaneously fitted to eq 6.

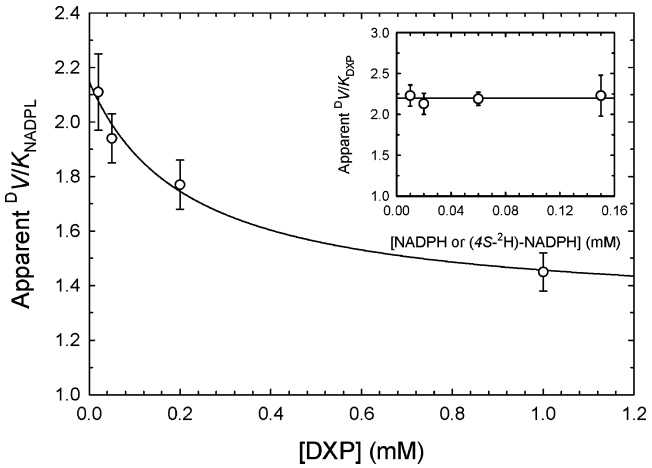

FIGURE 3: Dependence of the apparent values of $^D(V/K)_{NADPH}$ and $^D(V/K)_{DXP}$ on the concentration of the cosubstrate. Assays contained 100 mM Hepes, pH 7.5, 10 mM Mg^{2+}, *M. tuberculosis* DXP isomeroreductase, DXP, and NADPH or [4*S*-^{2}H]NADPH. The solid line drawn through the apparent $^D(V/K)_{NADPH}$ data is a fit to $^DV/K_{app} = {}^DV/K_{[DXP]\to\infty} + K[{}^DV/K_{[DXP]\to 0} - {}^DV/K_{[DXP]\to\infty}]/(K + [DXP])$, where K is the concentration of DXP that gives $^DV/K_{app} = [{}^DV/K_{[DXP]\to 0} + {}^DV/K_{[DXP]\to\infty}]/2$.

Cook and Cleland (*24*) have developed the theory of isotope effects for multireactant enzymes. In the following discussion, A and B refer to the substrate that binds to the enzyme first and second, respectively, if the mechanism is ordered. Isotope effects will be observed on *V*/*K* for both A and B, regardless of which substrate carries the heavy isotope, in the present case, a deuterium atom on the C_4-*proS* position of the dihydronicotinamide ring of the reduced pyridine nucleotide. For steady-state mechanisms, $^D(V/K_{app})$ for one substrate will vary with the concentration of the cosubstrate depending on whether the mechanism is ordered or random. In steady-state ordered mechanisms, $^D(V/K_{app})_B$ will be independent of the concentration of A, while $^D(V/K_{app})_A$ will decrease as the concentration of B is increased and become unity at infinite concentration of B, if A is sticky. In steady-state random mechanisms, $^D(V/K_{app})$ for a sticky substrate will decrease as the concentration of the cosubstrate is increased and reach a nonunitary finite value at infinite concentration of the cosubstrate, whereas for a nonsticky substrate, $^D(V/K_{app})$ will be independent of the concentration of the cosubstrate. Finally, for rapid equilibrium mechanisms, whether ordered or random, $^D(V/K)$ for the two substrates will be equal and independent of the concentration of the cosubstrate because all external commitment factors are zero.[4]

Table 4: Primary Deuterium Kinetic Isotope Effects (NAD(P)H vs [4*S*-^{2}H]NAD(P)H) for *M. tuberculosis* DXP Isomeroreductase[a]

metal ion	pyridine nucleotide	$^DV/K_{PyrNuc}$	$^DV/K_{DXP}$	^DV
Mg^{2+}	NADPH	1.3 ± 0.1	2.2 ± 0.1	1.3 ± 0.1
Mg^{2+}	NADH	[b]	[b]	[b]
Mn^{2+}	NADPH	1.3 ± 0.1	2.9 ± 0.2	2.2 ± 0.1
Mn^{2+}	NADH	2.9 ± 0.4	4.8 ± 0.8	2.9 ± 0.3
Co^{2+}	NADPH	0.9 ± 0.1	1.1 ± 0.1	1.2 ± 0.1
Co^{2+}	NADH	1.2 ± 0.3	1.7 ± 0.4	1.8 ± 0.2

[a] At pH 7.5 and 25 °C. [b] Not determined due to the large errors associated with the NADH and DXP kinetic parameters (see Table 2).

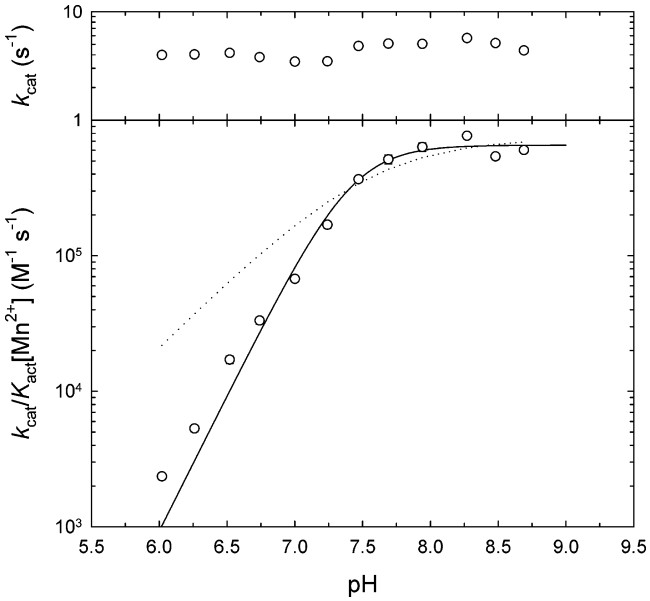

FIGURE 4: Dependence of k_{cat} and $k_{cat}/K_{act}^{Mn^{2+}}$ on pH at saturating levels of DXP and NADPH. The following buffers were used (100 mM): Mes, $6.00 \le$ pH ≤ 6.50; Hepes, $6.75 \le$ pH ≤ 8.00; Taps, $8.25 \le$ pH ≤ 8.75. The dotted and solid lines are fits to eqs 7 and 8, respectively.

While $^D(V/K_{app})_{DXP}$ is independent of the concentration of NADPH, $^D(V/K_{app})_{NADPH}$ decreases as the concentration of DXP is increased (Figure 3). The solid line drawn through the $^D(V/K_{app})_{NADPH}$ data is a fit to a hyperbola, giving a limiting value of 1.3 ± 0.1 for $^D(V/K)_{NADPH}$ at infinite concentration of DXP. These results are inconsistent with

[3] A substrate is "sticky" if it reacts to give products as fast or faster than it dissociates from the enzyme. In such cases the external portion of the commitment factor[4] is large, which depresses isotope effects from the intrinsic value (*24*).

[4] Commitment factors have external and internal portions. External portions arise from sticky substrates. Internal portions may arise from chemical steps other than the one being probed, such as the isomerization step (Scheme 2), and enzyme conformational changes (*24*).

an ordered mechanism with DXP binding first, as was suggested by the above product inhibition studies, because $^{D}(V/K_{app})_{DXP}$ does not vary with the level of NADPH. Since both $NADP^+$ and MEP are noncompetitive inhibitors with respect to NADPH, a strictly ordered mechanism with NADPH binding first is also unlikely. The isotope effect results, however, are fully consistent with a random mechanism in which either substrate can bind to the enzyme regardless of whether the cosubstrate is bound or not. However, the data do not rule out a preferred order of substrate addition, which would be dictated by the affinity of the enzyme for NADPH relative to DXP. The significantly lower K_m value for NADPH relative to DXP, for example (see Table 2), would favor a preferred order of addition of NADPH followed by DXP. This proposal would be in agreement with the results of dead-end inhibition studies performed on the *E. coli* DXP isomeroreductase, where an ordered mechanism with NADPH binding first was proposed (*29*). As will be elaborated on later, the results also demonstrate that NADPH is significantly more sticky than DXP.

For ordered mechanisms, the steady-state kinetic parameters for the forward and reverse reactions are related to the equilibrium constant by the following expression (*36*), where A binds to the enzyme before B, and P is released from the enzyme before Q:

$$K_{eq}' = \frac{k_{cat}^{f}}{k_{cat}^{r}}\left(\frac{K_{iq}K_m^{P}}{K_{ia}K_m^{B}}\right)$$

As a check for internal consistency, the right-hand side of the above expression, which is composed of steady-state kinetic constants, should be equal to the equilibrium constant (K_{eq}') of the reaction, determined from an independent experiment. If A = NADPH, B = DXP, P = MEP, and Q = $NADP^+$, the calculated value of K_{eq}' is 26 ± 9, which is in reasonable agreement with the value of 52 that we determined independently (data not shown). This K_{eq}' value is similar to the values of 46 (*29*) and 69 (*17*),[5] which were determined for the *E. coli* enzyme at the same pH. For random mechanisms, the same relationship applies, and one can assume either order of substrate addition (*36*). If A = DXP, B = NADPH, P = $NADP^+$, and Q = MEP, the calculated value of K_{eq}' is 27 ± 14. These results are also consistent with a random mechanism, since the same calculated value of K_{eq}' is obtained regardless of the assumed order of substrate addition.

The structures of a metal-free E·NADPH complex (*37*) and of an E·Mn^{2+}·fosmidomycin complex (*38*) have been solved for the *E. coli* DXP isomeroreductase by X-ray crystallography. This is additional evidence that supports a random mechanism because the enzyme can bind NADPH regardless of whether metal and fosmidomycin, which mimics DXP (*38*), are bound and vice versa. It should be noted that, in the absence of rapid equilibrium segments, all product inhibition patterns in steady-state random mechanisms are expected to be noncompetitive (*35*). The observation that $^{D}(V/K_{app})_{DXP}$ is independent of the concentration of NADPH demonstrates that DXP is not sticky and suggests that rapid equilibrium segments exist. This may account for the single competitive inhibition pattern that was observed (MEP versus DXP, Table 3).

Magnitude of the Isotope Effects Depends on Metal Ion Identity. The magnitude of isotope effects in enzymatic reactions is usually smaller than the intrinsic value due to high commitment factors. Altering the pH of the reaction (*39*, *40*) or selecting less sticky substrate analogues are two commonly employed methods of lowering the external portion of the commitment factors, thereby increasing the observed isotope effect. Here we show that the identity of the metal ion activator can also alter the commitment factors and, hence, the magnitude of the observed isotope effects. For example, with NADPH as the reductant, the $^{D}V/K_{DXP}$ values decrease from 2.9 to 2.2 to 1.1 for Mn^{2+}, Mg^{2+}, and Co^{2+}, respectively (Table 4). A similar comparison can be made for the $^{D}V/K_{NADPH}$ values. To our knowledge, this is only the second demonstration of significant differences in the magnitude of isotope effects with different metal ion activators, the other being the NAD^+-specific malic enzyme from *Ascaris suum* (*41*).

It was also possible that the differential magnitude of the isotope effects was due to different enzymatic mechanisms with the different metal ions. For example, as an alternative to the generally accepted 2-hydroxy-1-phosphoethyl shift mechanism (middle pathway, Scheme 2), a retroaldolization/aldolization mechanism recently considered by Rohmer and co-workers (*17*) (upper pathway, Scheme 2) and a sequential 1,2-hydride and 1,2-methyl shift mechanism (lower pathway, Scheme 2), which to our knowledge has not been considered in the literature, also seemed possible. We synthesized 2-[^{13}C]DXP, converted it to the product MEP with *M. tuberculosis* DXP isomeroreductase, purified it, and carried out ^{13}C NMR to determine the position of the ^{13}C label (Experimental Procedures). The ^{13}C label ended up *exclusively* at the 2-position of MEP regardless of the metal ion activator used (data not shown). Thus, the sequential 1,2-hydride and 1,2-methyl shift mechanism does not appear to occur with any metal ion (see Scheme 2). The other two mechanisms are expected to give the same ^{13}C product profile and hence cannot be distinguished by this method. Similar labeling experiments with the *E. coli* enzyme also showed a ^{13}C product profile consistent with both of these mechanisms (*17*, *42*). Until methods are developed to distinguish between these two possibilities, we tentatively conclude (1) that the enzymatic mechanism is likely the same regardless of metal ion identity and (2) that the differences in the magnitude of the observed isotope effects are most likely due to differences in commitment factors.

With Mn^{2+} and Mg^{2+}, the $^{D}V/K_{DXP}$ values of 2.9 and 2.2, respectively, were higher than the corresponding $^{D}V/K_{NADPH}$ values of 1.3 because NADPH is significantly more sticky than DXP. With Co^{2+}, no significant isotope effects on $^{D}V/K_{DXP}$ and $^{D}V/K_{NADPH}$ were observed, probably because both substrates are very sticky with this metal ion.

The magnitude of these isotope effects is expected to increase when a less sticky substrate is used because the external portion of the commitment factors will become smaller. While the k_{cat} values did not change significantly when NADH was used in place of NADPH, the K_m value for NADH relative to NADPH increased about 100-fold

[5] This K_{eq}' value was calculated from the value of 2.2×10^9 M^{-1} for K_{eq} (*17*) and the relationship $K_{eq}' = K_{eq}[H^+]$, where $[H^+] = 3.2 \times 10^{-8}$ M at pH 7.5.

(Table 2), suggesting that the 2′-phosphate of NADPH contributes mostly to binding and not to catalysis. The K_m value for DXP also increased, 2.5−10-fold, depending on the metal ion activator that was used. It has been reported for the *Zymomonas mobilis* (*28*) and *Synechocystis* sp. PCC6803 (*26*) DXP isomeroreductases that no activity could be detected with NADH, and that NADH gives only 1% of the activity of NADPH for the *E. coli* (*12*, *27*) enzyme, contrary to our results with the *M. tuberculosis* enzyme, where the k_{cat} values are similar with these two reduced pyridine nucleotides. Our results with the *M. tuberculosis* enzyme provide an explanation for this discrepancy. We think that in these earlier studies the enzyme was not saturated with the substrates because of the high K_m values for the NADH and DXP substrate pair.

Since NADH seemed to fit the criteria for a less sticky substrate relative to NADPH, we repeated the isotope effects using [4*S*-^{2}H]NADH. As anticipated, the isotope effects on *V*/*K* for both substrates increased significantly. Though the isotope effects have clearly increased when Co^{2+} was the metal ion activator, the isotope effects remained relatively small, suggesting that the commitment factors are still large for the NADH and DXP substrate pair with this metal ion. With Mn^{2+} as activator, NADH and DXP are now almost completely nonsticky, resulting in a significantly lowered external commitment and permitting almost full expression of the intrinsic primary deuterium kinetic isotope effect.

Rate-Limiting Steps. Isotope effects have classically been used to probe whether a specific chemical step limits the rate of a reaction. For enzymatic reactions, isotope effects on *V*/*K* and *V* probe different portions of the reaction for rate-limiting chemical steps. Isotope effects on *V*/*K* probe all steps up to and including the first irreversible step, generally considered to be release of the first product. In the present case, the above isotope effects on *V*/*K* established that substrate binding and release, particularly that of NADPH, is slow compared to chemistry and that the rate of this binding/release step is further controlled by the metal ion activator.

Isotope effects on *V* probe all steps after the formation of the enzyme complex that will subsequently undergo catalysis: in the present case, the E·M^{2+}·DXP·NAD(P)H complex. In addition to the reduction step, the isomerization step leading to formation of **I**, enzyme conformational change(s), and product release steps are also probed. For DXP isomeroreductase, the magnitude of ^DV increases when NADH is used in place of NADPH, suggesting that release of at least one of the products or an enzyme conformational change(s) is at least partly rate-limiting with NADPH. As was the case with $^DV/K$, the magnitude of ^DV also depends on the identity of the metal ion activator. With NADPH, ^DV is higher for Mn^{2+} than for Mg^{2+} or Co^{2+}, suggesting that, relative to the reduction step, at least one of the steps listed above is slower for Mg^{2+} and Co^{2+} compared to Mn^{2+}. Transient-state kinetic experiments together with heavy-atom isotope effects are required to identify these slow steps.

Role of the Divalent Metal Ion in Catalysis. Deprotonation of a substrate hydroxyl group is required to initiate the isomerization step (see Scheme 2). The isomerization step could also be assisted by protonation of intermediates. If enzymatic group(s) or a metal-bound water/hydroxide molecule act as general base and acid catalysts, their pK_a values would have to be less than ∼5 and greater than ∼9.5, respectively, because k_{cat} is independent of pH in the region $6.0 \leq pH \leq 8.75$. It is more likely that the divalent metal ion has the dual role of (1) promoting the initial ionization of the substrate hydroxyl group and (2) assisting in the formation of intermediate(s), by stabilizing the alkoxide form of the substrate and intermediate hydroxyl groups via electrostatic interactions (see Scheme 2), because for such electrostatic catalysis k_{cat} is not expected to vary with pH.

While k_{cat} is pH-independent, the $K_{act}^{Mn^{2+}}$ value increases sharply from a value of 7 μM at pH 8.75 to 1.7 mM at pH 6.0, resulting in a pH−$k_{cat}/K_{act}^{Mn^{2+}}$ profile that decreases at low pH as two ionizable groups on the enzyme with similar pK_a values of 7.4 become protonated. We think that these deprotonated groups coordinate the metal ion in the active site. Insight into the nature of these groups is provided by the recent crystal structure of the *E. coli* DXP isomeroreductase with bound Mn^{2+} and fosmidomycin (*38*). Three carboxylate groups, which are conserved in DXP isomeroreductases from other species (D 151, E 153, and E 222, *M. tuberculosis* enzyme numbering), coordinate the Mn^{2+} via monodentate interactions. The aldehyde and hydroxyl groups of fosmidomycin and a water molecule are the remaining three ligands that coordinate the Mn^{2+}. Though the pK_a values of 7.4 that we obtained from these pH studies are high for carboxylate groups, the presence of three carboxylate groups in close proximity to one another is expected to substantially increase the pK_a values from their usual values, such that they are largely protonated at neutral pH unless a metal ion is bound.

CONCLUSIONS

We performed product inhibition and isotope effect experiments on DXP isomeroreductase from *M. tuberculosis* to determine its steady-state kinetic mechanism and to identify rate-limiting steps. The data rule out ping-pong and rapid equilibrium sequential mechanisms and are most compatible with a steady-state random mechanism. The magnitude of the isotope effects suggests that substrate stickiness, particularly that of NADPH, is strongly influenced by the identity of the metal ion. With Mn^{2+} as activator, this stickiness was almost completely removed when NADH replaced NADPH, permitting almost full expression of the intrinsic primary deuterium kinetic isotope effect. With the Co^{2+}-activated enzyme, the isotope effects were only partly unmasked when NADH replaced NADPH, suggesting that other steps, such as the isomerization step, may be partly rate-limiting with this metal ion. Finally, our pH studies support an electrostatic role for the divalent metal ion in catalysis.

REFERENCES

1. Sacchettini, J. C., and Poulter, C. D. (1997) Creating isoprenoid diversity, *Science 277*, 1788−1789.
2. Rohdich, F., Kis, K., Bacher, A., and Eisenreich, W. (2001) The nonmevalonate pathway of isoprenoids: genes, enzymes and intermediates, *Curr. Opin. Chem. Biol. 5*, 535−540.
3. Rodriguez-Concepcion, M., and Boronat, A. (2002) Elucidation of the methylerythritol phosphate pathway for isoprenoid biosynthesis in bacteria and plastids. A metabolic milestone achieved through genomics, *Plant Physiol. 130*, 1079−1089.
4. Jomaa, H., Wiesner, J., Sanderbrand, S., Altincicek, B., Weidemeyer, C., Hintz, M., Turbachova, I., Eberl, M., Zeidler, J.,

Lichtenthaler, H. K., Soldati, D., and Beck, E. (1999) Inhibitors of the nonmevalonate pathway of isoprenoid biosynthesis as antimalarial drugs, *Science 285*, 1573−1576.
5. Wiesner, J., Hintz, M., Altincicek, B., Sanderbrand, S., Weidemeyer, C., Beck, E., and Jomaa, H. (2000) *Plasmodium falciparum*: detection of the deoxyxylulose 5-phosphate reductoisomerase activity, *Exp. Parasitol. 96*, 182−186.
6. Sprenger, G. A., Schorken, U., Wiegert, T., Grolle, S., de Graaf, A. A., Taylor, S. V., Begley, T. P., Bringer-Meyer, S., and Sahm, H. (1997) Identification of a thiamin-dependent synthase in *Escherichia coli* required for the formation of the 1-deoxy-D-xylulose 5-phosphate precursor to isoprenoids, thiamin, and pyridoxol, *Proc. Natl. Acad. Sci. U.S.A. 94*, 12857−12862.
7. Cane, D. E., Du, S., Robinson, J. K., Hsiung, Y., and Spencer, I. D. (1999) Biosynthesis of vitamin B_6: enzymatic conversion of 1-deoxy-D-xylulose-5-phosphate to pyridoxal phosphate, *J. Am. Chem. Soc. 121*, 7722−7723.
8. Laber, B., Maurer, W., Scharf, S., Stepusin, K., and Schmidt, F. S. (1999) Vitamin B_6 biosynthesis: formation of pyridoxine 5′-phosphate from 4-(phosphohydroxy)-L-threonine and 1-deoxy-D-xylulose-5-phosphate by PdxA and PdxJ protein, *FEBS Lett. 449*, 45−48.
9. Settembre, E., Begley, T. P., and Ealick, S. E. (2003) Structural biology of enzymes of the thiamin biosynthesis pathway, *Curr. Opin. Struct. Biol. 13*, 739−747.
10. Kuzuyama, T., Shimizu, T., Takahashi, S., and Seto, H. (1998) Fosmidomycin, a specific inhibitor of 1-deoxy-D-xylulose 5-phosphate reductoisomerase in the nonmevalonate pathway for terpenoid biosynthesis, *Tetrahedron Lett. 39*, 7913−7916.
11. Missinou, M. A., Borrmann, S., Schindler, A., Issifou, S., Adegnika, A. A., Matsiegui, P. B., Binder, R., Lell, B., Wiesner, J., Baranek, T., Jomaa, H., and Kremsner, P. G. (2002) Fosmidomycin for malaria, *Lancet 360*, 1941−1942.
12. Takahashi, S., Kuzuyama, T., Watanabe, H., and Seto, H. (1998) A 1-deoxy-D-xylulose 5-phosphate reductoisomerase catalyzing the formation of 2-*C*-methyl-D-erythritol 4-phosphate in an alternative nonmevalonate pathway for terpenoid biosynthesis, *Proc. Natl. Acad. Sci. U.S.A. 95*, 9879−9884.
13. Rodriguez-Concepcion, M., Campos, N., Maria Lois, L., Maldonado, C., Hoeffler, J. F., Grosdemange-Billiard, C., Rohmer, M., and Boronat, A. (2000) Genetic evidence of branching in the isoprenoid pathway for the production of isopentenyl diphosphate and dimethylallyl diphosphate in *Escherichia coli*, *FEBS Lett. 473*, 328−332.
14. Kobayashi, K., Ehrlich, S. D., Albertini, A., Amati, G., Andersen, K. K., Arnaud, M., Asai, K., Ashikaga, S., Aymerich, S., Bessieres, P., et al. (2003) Essential *Bacillus subtilis* genes, *Proc. Natl. Acad. Sci. U.S.A. 100*, 4678−4683.
15. Rohmer, M., Knani, M., Simonin, P., Sutter, B., and Sahm, H. (1993) Isoprenoid biosynthesis in bacteria: a novel pathway for the early steps leading to isopentenyl diphosphate, *Biochem. J. 295* (2), 517−524.
16. Rohmer, M., Seemann, M., Horbach, S., Bringer-Meyer, S., and Sahm, H. (1996) Glyceraldehyde 3-phosphate and pyruvate as precursors of isoprenic units in an alternative nonmevalonate pathway for terpenoid biosynthesis, *J. Am. Chem. Soc. 118*, 2564−2566.
17. Hoeffler, J. F., Tritsch, D., Grosdemange-Billiard, C., and Rohmer, M. (2002) Isoprenoid biosynthesis via the methylerythritol phosphate pathway. Mechanistic investigations of the 1-deoxy-D-xylulose 5-phosphate reductoisomerase, *Eur. J. Biochem. 269*, 4446−4457.
18. Smith, P. K., Krohn, R. I., Hermanson, G. T., Mallia, A. K., Gartner, F. H., Provenzano, M. D., Fujimoto, E. K., Goeke, N. M., Olson, B. J., and Klenk, D. C. (1985) Measurement of protein using bicinchoninic acid, *Anal. Biochem. 150*, 76−85.
19. Taylor, S. V., Vu, L. D., and Begley, T. P. (1998) Chemical and enzymatic synthesis of 1-deoxy-D-xylulose-5-phosphate, *J. Org. Chem. 63*, 2375−2377.
20. Radykewicz, T., Rohdich, F., Wungsintaweekul, J., Herz, S., Kis, K., Eisenreich, W., Bacher, A., Zenk, M. H., and Arigoni, D. (2000) Biosynthesis of terpenoids: 1-deoxy-D-xylulose-5-phosphate reductoisomerase from *Escherichia coli* is a class B dehydrogenase, *FEBS Lett. 465*, 157−160.
21. Chen, P. S., Toribara, T. Y., and Warner, H. (1956) Microdetermination of phosphorus, *Anal. Chem. 28*, 1756−1758.
22. Ottolina, G., Riva, S., Carrea, G., Danieli, B., and Buckmann, A. F. (1989) Enzymatic synthesis of [4*R*-^{2}H]NAD(P)H and [4*S*-^{2}H]-NAD(P)H and determination of the stereospecificity of 7 alpha- and 12 alpha hydroxysteroid dehydrogenase, *Biochim. Biophys. Acta 998*, 173−178.
23. Orr, G. A., and Blanchard, J. S. (1984) High-performance ion-exchange separation of oxidized and reduced nicotinamide adenine dinucleotides, *Anal. Biochem. 142*, 232−234.
24. Cook, P. F., and Cleland, W. W. (1981) Mechanistic deductions from isotope effects in multireactant enzyme mechanisms, *Biochemistry 20*, 1790−1796.
25. Skoog, D. A., and West, D. M. (1982) *Fundamentals of Analytical Chemistry*, pp 75−80, Saunders College Publishing, Philadelphia, PA.
26. Yin, X., and Proteau, P. J. (2003) Characterization of native and histidine-tagged deoxyxylulose 5-phosphate reductoisomerase from the cyanobacterium *Synechocystis* sp. PCC6803, *Biochim. Biophys. Acta 1652*, 75−81.
27. Kuzuyama, T., Takahashi, S., Watanabe, H., and Seto, H. (1998) Direct formation of 2-*C*-methyl-D-erythritol 4-phosphate from 1-deoxy-D-xylulose 5-phosphate by 1-deoxy-D-xylulose 5-phosphate reductoisomerase, a new enzyme in the nonmevalonate pathway to isopentenyl diphosphate, *Tetrahedron Lett. 39*, 4509−4512.
28. Grolle, S., Bringer-Meyer, S., and Sahm, H. (2000) Isolation of the *dxr* gene of *Zymomonas mobilis* and characterization of the 1-deoxy-D-xylulose 5-phosphate reductoisomerase, *FEMS Microbiol. Lett. 191*, 131−137.
29. Koppisch, A. T., Fox, D. T., Blagg, B. S., and Poulter, C. D. (2002) *E. coli* MEP synthase: steady-state kinetic analysis and substrate binding, *Biochemistry 41*, 236−243.
30. Alatossava, T., Jutte, H., Kuhn, A., and Kellenberger, E. (1985) Manipulation of intracellular magnesium content in polymyxin B nonapeptide-sensitized *Escherichia coli* by ionophore A23187, *J. Bacteriol. 162*, 413−419.
31. Frausto da Silva, J. J. R., and Williams, R. J. P. (1991) *The Biological Chemistry of the Elements. The Inorganic Chemistry of Life*, p 379, Clarendon Press, Oxford, U.K.
32. D'Souza V, M., and Holz, R. C. (1999) The methionyl aminopeptidase from *Escherichia coli* can function as an iron(II) enzyme, *Biochemistry 38*, 11079−11085.
33. Proteau, P. J., Woo, Y.-H., Williamson, T., and Phaosiri, C. (1999) Stereochemistry of the reduction step mediated by 1-deoxy-D-xylulose 5-phosphate isomeroreductase, *Org. Lett. 1*, 921−923.
34. Segel, I. H. (1975) *Enzyme Kinetics. Behavior and Analysis of Rapid Equilibrium and Steady-State Enzyme Systems*, p 323, John Wiley & Sons, Inc., New York.
35. Segel, I. H. (1975) *Enzyme Kinetics. Behavior and Analysis of Rapid Equilibrium and Steady-State Enzyme Systems*, pp 653−655, John Wiley & Sons, Inc., New York.
36. Cleland, W. W. (1982) An analysis of Haldane relationships, *Methods Enzymol. 87*, 366−369.
37. Yajima, S., Nonaka, T., Kuzuyama, T., Seto, H., and Ohsawa, K. (2002) Crystal structure of 1-deoxy-D-xylulose 5-phosphate reductoisomerase complexed with cofactors: implications of a flexible loop movement upon substrate binding, *J. Biochem. (Tokyo) 131*, 313−317.
38. Steinbacher, S., Kaiser, J., Eisenreich, W., Huber, R., Bacher, A., and Rohdich, F. (2003) Structural basis of fosmidomycin action revealed by the complex with 2-C-methyl-D-erythritol 4-phosphate synthase (IspC). Implications for the catalytic mechanism and antimalaria drug development, *J. Biol. Chem. 278*, 18401−18407.
39. Cook, P. F., and Cleland, W. W. (1981) pH variation of isotope effects in enzyme-catalyzed reactions. 1. Isotope- and pH-dependent steps the same, *Biochemistry 20*, 1797−1805.
40. Cook, P. F., and Cleland, W. W. (1981) pH variation of isotope effects in enzyme-catalyzed reactions. 2. Isotope-dependent step not pH dependent. Kinetic mechanism of alcohol dehydrogenase, *Biochemistry 20*, 1805−1816.
41. Karsten, W. E., Gavva, S. R., Park, S. H., and Cook, P. F. (1995) Metal ion activator effects on intrinsic isotope effects for hydride transfer from decarboxylation in the reaction catalyzed by the NAD-malic enzyme from *Ascaris suum*, *Biochemistry 34*, 3253−3260.
42. Hecht, S., Wungsintaweekul, J., Rohdich, F., Kis, K., Radykewicz, T., Schuhr, C. A., Eisenreich, W., Richter, G., and Bacher, A. (2001) Biosynthesis of terpenoids: Efficient multistep biotransformation procedures affording isotope-labeled 2*C*-methyl-D-erythritol 4-phosphate using recombinant 2*C*-methyl-D-erythritol 4-phosphate synthase, *J. Org. Chem. 66*, 7770−7775.

BI049974K